Frontiers in Scientific Research and Technology

Online ISSN: 2682-2970
Print ISSN: 2682-2962
http://fsrt.journals.ekb.eg

FSRT J 9 (2024) 35 - 47 10.21608/FSRT.2024.286795.1126

The reservoir potential of Middle Jurassic sedimentary deposits in the Imhotep Field, Matruh Basin, North-Western Egypt

Walaa A. Ali*

Petroleum Geology Department, Faculty of Petroleum and Mining Sciences, Matrouh University, 51511, Matrouh, Egypt

ARTICLE INFO

Article history:
Received 2 May 2024
Received in revised form 16 May 2024
Accepted 17 May 2024
Available online 25 May 2024

Keywords
reservoir potential,
geomechanics,
Imhotep Field,
Khatatba Formation,
Egypt.

ABSTRACT

This study examines the reservoir potential of the Middle Jurassic Khatatba Formation in the significant gas producer Imhotep Field, Matruh Basin, northwestern Egypt. The Upper Safa member sandstones of Khatatba Fm are characterized by low-quality, confined sandstone reservoirs. Yet, the Lower Safa member sandstones show better gas reservoir quality and exhibit remarkable decreases in shale volumes, including kaolinite. There is about a 30 m gross thickness, a 10 m net effective pay, about 6 % average effective porosity, 21% mD permeability, 12% shale volume, 24% water saturation and ~77% average hydrocarbon saturation. The deeply seated Lower Safa sandstone reservoirs in the Imhotep W-1X well are not suitable for gas production because they show a high decline in production and pressure tests. Therefore, they require high pressure to produce gas and condensates, which is probably not economically feasible. Moreover, geomechanical results indicate that the Lower Safa member is a brittle reservoir with better drilling capabilities than the more ductile Upper Safa member. Because of the vertical facies change and sandstone low-permeability in the Khatatba Fm, the quality of the reservoir is seen as the biggest risk that was tested in the field. In general, the Khatatba Fm in the Imhotep Field is a better reservoir because it is mostly made up of coarse, organically poor clastic deposits in the Imhotep W-1X well area. More studies based on multi-approach analysis are needed to fully examine the regional reservoir potential of the Khataba Fm in the Matruh Basin.

1. Introduction

The Matruh Basin, located in northwestern Egypt, holds approximately 23 billion barrels of oil (BBOE) and 3 trillion cubic feet (TCF) of gas reserves. The main Mesozoic source rocks in the basin are the Middle Jurassic Khatatba, Lower Cretaceous Alam El Bueib, and Upper Cretaceous “G” Member of the Abu Roash formations. The Matruh Basin's petroleum system has proven to generate oil and gas, reaching the final phase of hydrocarbon generation (El-Shorbagy et al., 2023a, b). The Study of (Shalaby et al., 2012), have suggested that the Khatatba Formation's shales and coaly shales in the Shams SE-1 and Shams NE-1 wells in the Shushan Basin are late mature to early overmature, poor to excellent gas-prone source rocks. El Nady et al., (2016) studied the dark gray shales and carbonates of the upper Khatatba Formation in the Salam-3X and fair mature gas-prone source rocks in the Shushan Basin. Gentzis et al., (2018) found a thick carbonate section (390 m) with only a few shale horizons of the Khatatba Formation in northeast Matruh Basin through the Abu Tunis-1X well as a reservoir rock containing migrated hydrocarbons and NSO compounds.

Aljahdali et al., (2023) suggested the intraformational shales of Khatatba Formation in the OBA D-17 well in in the Shushan Basin as good late mature oil source rocks. Recently, Ali and Fagelnour (2023), modeled the Middle Jurassic Khatatba Formation for hydrocarbon source rock potential in the Matruh Basin using geological and geochemical data from the Apidose-1X well. They concluded that the Matruh Basin includes all elements of the petroleum system, with generation, migration, and accumulation beginning in the Early Cretaceous. Moreover, Ali (2023), studied the Khatatba Formation in Matruh Field using organic and inorganic data from two wells and analyzed the provenance and sedimentation conditions for Middle Jurassic source rock deposits. Ali (2023) as well interpreted the formation as formed during sea regression, with the Upper and Lower Safa members being the most significant source rocks in the Matruh Field. This led to shallow marine sediment deposition. This work aims to evaluate the reservoir potential of the Khatatba Formation in the Imhotep Field, Matruh Basin, using petrophysical, and geomechanical analyses.

* Corresponding author at Matrouh University

E-mail addresses: walaa.ali@mau.edu.eg (Walaa A. Ali)

2. Geological setting and lithostratigraphy

The geological history and setting of the northern Desert of Egypt, reflect in part the tectonostratigraphic evolution of the Unstable Shelf, which represents the northeastern part of the African Craton (Fig. 1). The Western Desert's hydrocarbon occurrence is tightly tied to historical tectonic and stratigraphic events, which made multiple source, reservoir, and seal combinations. According to Metwalli et al., (2018), the northern section of Egypt witnessed three separate tectonic events. The initial event formed the NW or WNW fault trend during the Paleozoic–Early Mesozoic (Triassic). The second event happened during the Late Mesozoic (Cretaceous) and generated the ENE Syrian Arc System, which is built of a sequence of faulted anticlines of varied dips and directions. Finally, the third tectonic event developed throughout the Early Cenozoic (Late Eocene and Early Oligocene) and generated the NW Gulf of Suez and NNE Aqaba fault lines. Various geological studies dealt with the tectonic framework, stratigraphy, facies distribution, and development of sedimentary basins in the northwestern Desert (e.g., Meshref, 1999; Guiraud and Bosworth, 1999; Shalaby et al., 2012; EL Bastawesy et al., 2020; Bosworth and Tari, 2021; Deaf et al., 2022).

The deposition of the sedimentary sequence in the Matruh Basin was governed by the regional tectonics associated to the drift of the African plate and rifting of the Tethyan Ocean. This resulted in accumulation of thick sedimentary successions, which are split into four primary depositional sequences "DSQ" (Fig. 2). The investigated Khatatba Formation in the Imhotep W-1X well is characterized from the base to the top by clastics of the Lower Safa and Upper Safa members, with the carbonates of the Kabrit Member acting as a separating thick bed. The carbonates of the Zahra Member comprise the topmost section of the Khatatba Formation.

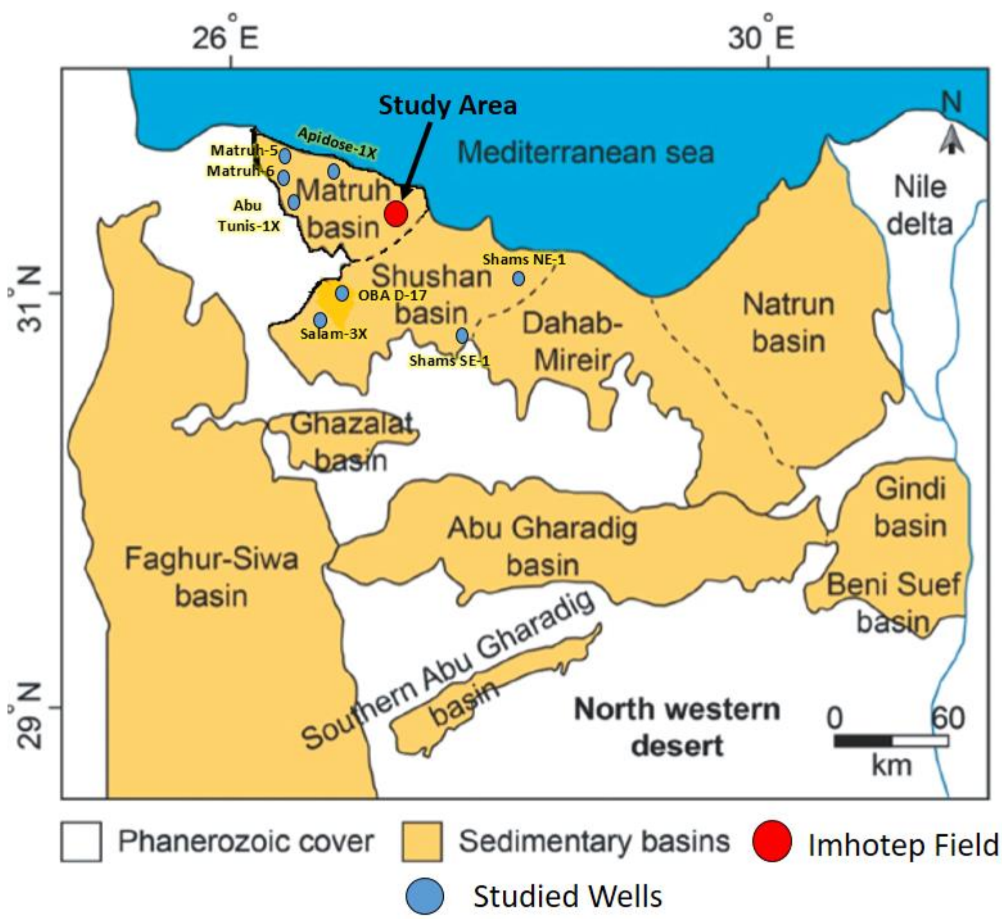

Fig. 1. Location map of the Matruh Basin along with other Mesozoic basins in the North Western Desert of Egypt and location of the studied Imhotep W-1X well (Modified after EGPC, 1992; Diab and Khalil, 2021).

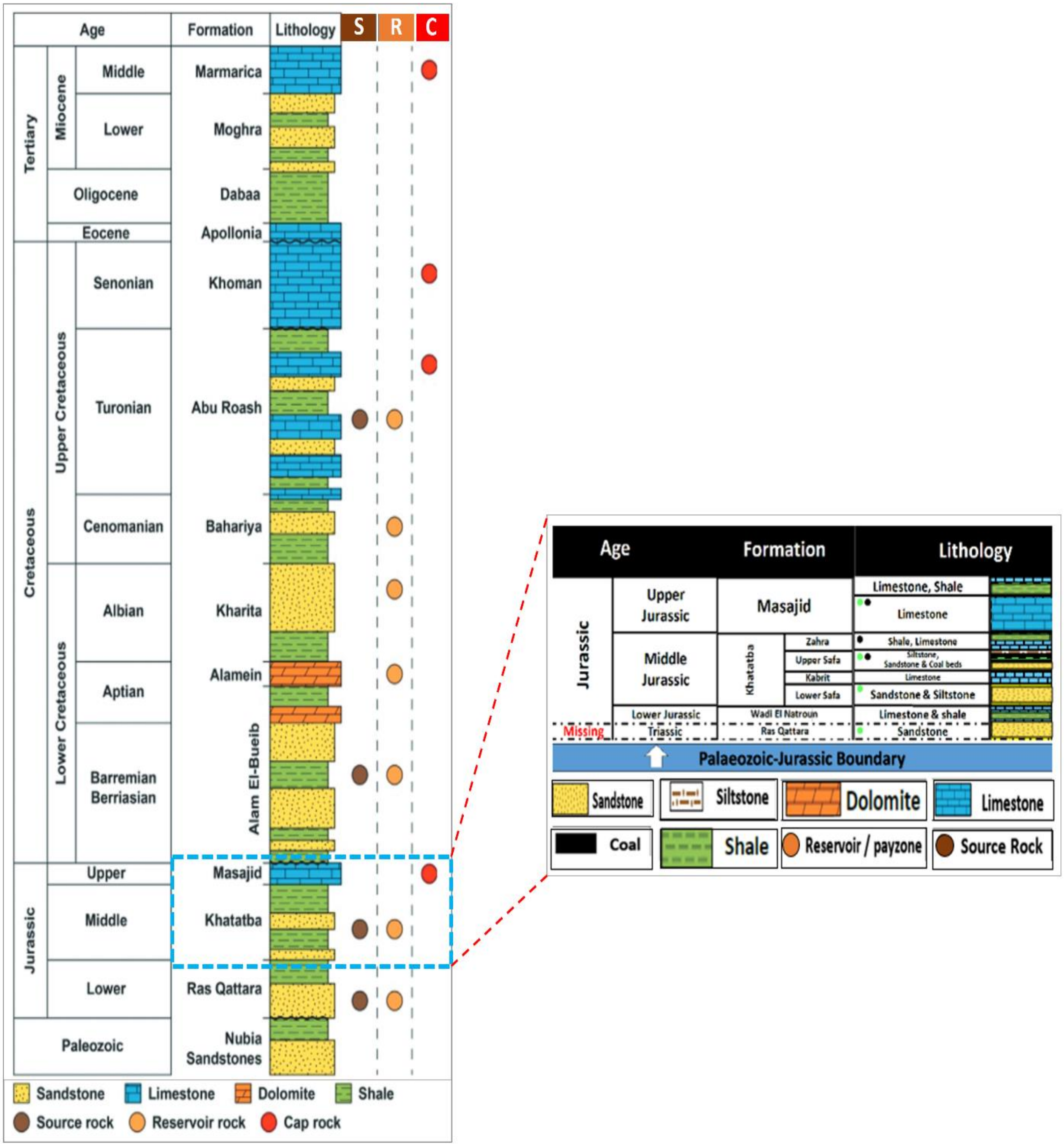

Fig. 2. Stratigraphic column of the Matruh Basin, North Western Desert, Egypt, showing main petroleum system elements with the lithology and age of the formations (modified after Abdou, 1998).

3. Methodology and analyses

3.1 Petrophysical analyses

Various types of geophysical data were analyzed to identify the lithology, organic richness, and petrophysical parameters of the Khatatba Formation intervals in the Imhotep W-1X well, as shown in the following subsection and in the workflow (Fig. 3). Lithology, volume of shale, porosity, and water saturation were determined following the methodology of Clavier et al., (1984), Asquith et al., (2004), Hakimi et al., (2012), Al-Areeq and Alaug (2014), Osli et al., (2018), and Deaf et al., (2022).

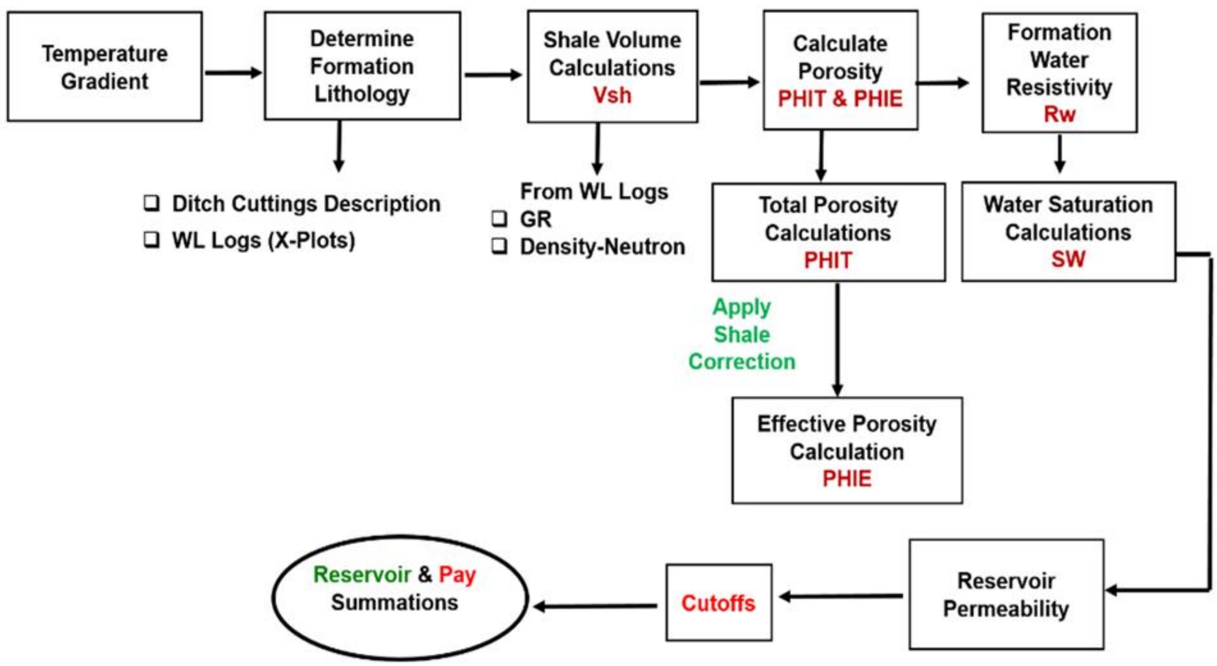

Fig. 3. A workflow chart showing the steps of analysis used in the petrophysical evaluation of the Khatatba Formation reservoirs in the Imhotep W-1X well, the Matruh Basin, Egypt.

3.2. Hydrocarbon mobility

Schlumberger (1972), found that the ratio (S_w / S_{xo}) is a reliable indicator of oil mobility. If it equals 1, it suggests no hydrocarbons have been displaced due to invasion. However, a value of 0.7 or lower suggests hydrocarbon presence. The ratio can be calculated using the formula $(S_w / S_{xo})^2 = (R_{xo} / R_t) / (R_{mf} / R_w)$.

3.3. Rock geomechanics methodology

Rock mechanical characteristics are crucial for determining the quality, strength, and potential of a rock. Well logging techniques are used to determine these characteristics, which are calibrated with core data if available. Shale brittleness is a key outcome, and shale intervals with high brittleness levels are ideal for identifying hydraulic fracture initiation. Geomechanical models can enhance brittleness estimation and optimize parameters like perforation intervals, fracture pressure, and geometry. To start the geomechanical analysis, data for density, porosity, compressional, slowness, and volume of shale are evaluated and checked for quality. If density tools are unavailable, synthetic logs can be generated using workflow diagrams (Fig.4). Mechanical rock parameters like Poisson's ratio (PR) and Young's modulus (YM) are often derived from well logs. Brittleness is a function of two key rock properties: Poisson's ratio (PR) and Young's modulus (YM), indicating the rock's susceptibility to failure (Rickman et al., 2008).

The brittleness of a formation increases with the increase in YM value and decrease in PR value, leading to increased fracturing and reduced stress. In contrast, ductile shale intervals exhibit more plasticity and require elevated pressure for fracturing (Perez Altamar and Marfurt, 2014).

Rocks with brittle characteristics have a wider range of elastic behavior and a narrower range of ductile behavior. Shale reservoirs have low porosity and permeability, ranging from 4% to 6.5%, and act as a source, reservoir, and seal in a shale gas system (Sander et al., 2017). Shale gas reservoirs are suitable for commercial exploitation when they have a brittleness index of over 40%, facilitating more effective fracturing (Zou et al., 2021). Following the procedure described by Jaeger et al. (2009), Schön (2015), Wu and Grana (2017), and Kinppel et al. (2023), a workflow has been established in Figure 3 to illustrate the equations used to estimate the rock mechanics for petrophysics from well logs.

4. Results and Interpretations

4.1. Reservoir Petrophysical evaluation

The litho-saturation plot of the Lower Safa Member shows that the rock type is mostly made up of shale layers, sandstone bodies with some calcareous cement, a few limestone horizons, and very small coal streaks. The Upper Safa Member consists primarily of shale, with siltstone intercalations as a major lithological constituent. Additionally, it contains sandstone horizons with calcareous cement as well as occasional limestone beds and coal streaks.

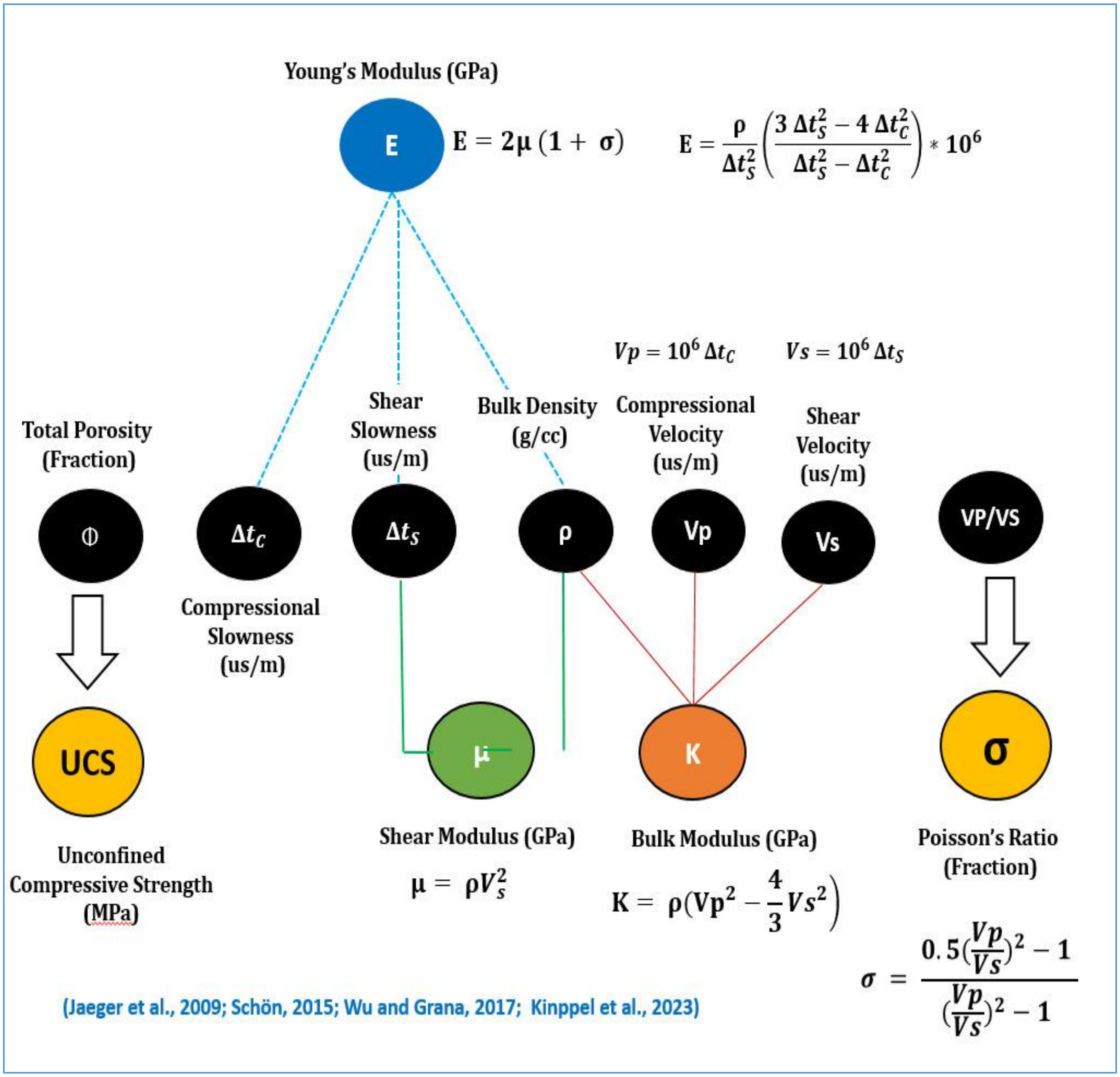

Fig. 4. The workflow of the rock mechanics assessment and used equations to detect the brittle and ductile intervals in the Khatatba Formation in the Imhotep W-1X well.

The volume of shale (Vsh) was calculated in front of sand intervals using the GR-method, the neutron density (ND), and the combined method of NS, Res, and SD. The ND-method shows the best results in front of the sand reservoirs of the Lower and Upper Safa Members, where the Lower Safa Member has a Vsh of 8% using the ND-method and 12% using the GR-method, while the Upper Safa Member has a Vsh of 25% using the ND-method and 38% using the GR-method. It is obvious from Table 1 below that the GR method overestimated the Vsh of the Lower and Upper Safa members in front of sand reservoirs.

In the case of the Lower Safa Member (Fig. 5), it is evident from track 3 (Sw/Sxo) that there is an absence of mobile hydrocarbons in the sand intervals. However, the recovery factor indicates that these intervals are filled with gas. This phenomenon can be attributed to the fact that the capillary pressure exceeds the buoyancy pressure of the hydrocarbon. The company's pressure test, which produced negative results in the Lower Safa Member, further supports the veracity of this claim. Thus, the Lower Safa Member was isolated, where production was made from the Alam El Bueib unit- 6 (AEB-6).

Table 1. The calculated volume of shale (Vsh) for the Khtatba Formation units (Lower Safa, Upper Safa, and Zahra members) using the GR-method (Vsh_GR), the Neutron-Density (ND) method (Vsh_ND), the Neutron-Sonic method (Vsh_NS), the resistivity method (Vsh_R), and the Sonic-Density method (Vsh_SD).

Zone	Lithology	Vsh_GR	Vsh_ND	Vsh_NS	Vsh_R	Vsh_SD
ZAHRA	SAND	0.30	0.38	**0.09**	1.00	0.27
	SILT	0.79	0.72	0.01	0.99	0.45
	SHALE	0.77	0.72	0.01	0.97	0.32
UPPER SAFA	SAND	0.38	**0.25**	0.37	1.00	**0.25**
	SILT	0.73	0.47	0.28	1.00	0.43
	SHALE	0.85	0.56	0.23	0.98	0.38
LOWER SAFA	SAND	0.12	**0.08**	0.65	1.00	0.28
	SILT	0.67	0.39	0.45	0.99	0.46
	SHALE	0.87	0.42	0.17	0.94	0.27

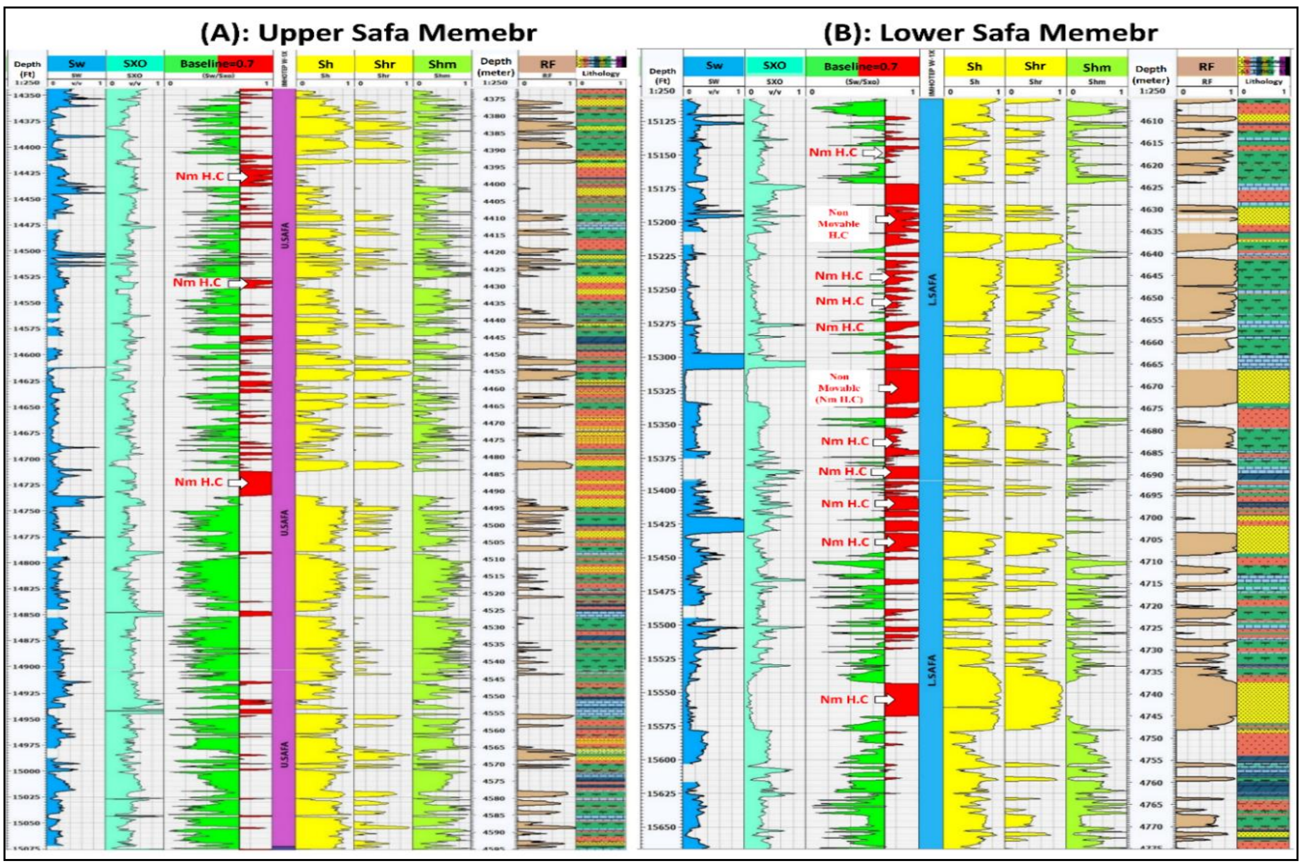

Fig.5. Petrophysical evaluation of (A): the Upper Safa, and (B): Lower Safa member of the Khatatba Formation in the Imhotep W-1X well. Track 1: total water saturation (Sw), Track 2: water saturation of flushed zone (Sxo), Track 3: hydrocarbon mobility (S_w/Sxo), Track 4: hydrocarbon saturation (Sh), Track 5: residual hydrocarbon saturation (Shr), Track 6: movable hydrocarbon saturation (Shm), and Track 7: recovery factor (RF). The final track represents the formation lithology. Depth is illustrated in meters and feet.

For the Upper Safa Member, no pay was encountered since the petrophysical evaluation showed that there was no pay calculated due to the tightness of the present sandstone. The average shale volume in front of sand was high and attained 31% after the correction of shale and a high-water saturation, which attained 51%. The effective water saturation was about 46% after applying the Indochina equation, which takes into account the correction for the effect of shale. Moreover, the effective porosity is just 3.7%, which shows how tight the reservoir is (refer to the table provided in Fig. 6A). The geologists of the owner company confirm the findings of the petrophysical analysis (Personal Communications, 2024).

The comprehensive petrophysical analysis of the Lower Safa sandstone units reveals a total gross thickness of ~30m, within which about 10 m is considered as net effective pay. The average effective porosity was estimated to be around 6%, while the average water saturation is around 24%. Conversely, the average hydrocarbon saturation is calculated to be 77%, with an average shale volume of approximately 12% from the GR log and 8% from the ND logs. One issue pertaining to gas reservoirs is that as the depth of the reservoir increases, a correspondingly higher pressure is required for extraction purposes. In general, the petrophysical assessment categorizes the Lower Safa Member as a favorable gas reservoir, as shown by the determined petrophysical data (see tabulated data provided in base of (Fig. 6B).

The primary porosity was estimated from the sonic log to be ~16.35% in the Lower Safa and ~18.13% in the Upper Safa members. The secondary porosity was estimated by subtracting the total porosity computed from the Neutron-Density logs and from the porosity derived from sonic log. It is observed that diagenesis played a major role in controlling the reservoir quality, where the secondary porosity was estimated to be 9.51% in the Lower Safa member, which is higher than that of the Upper Safa member 7.69%. This may be related to the effect of digenesis, which is higher in the Lower Safa and probably created several secondary pore spaces with better permeability characteristics for fluid transmission and accumulation as a result of compaction due to the Lower Safa deep burial (Fig. 6B).

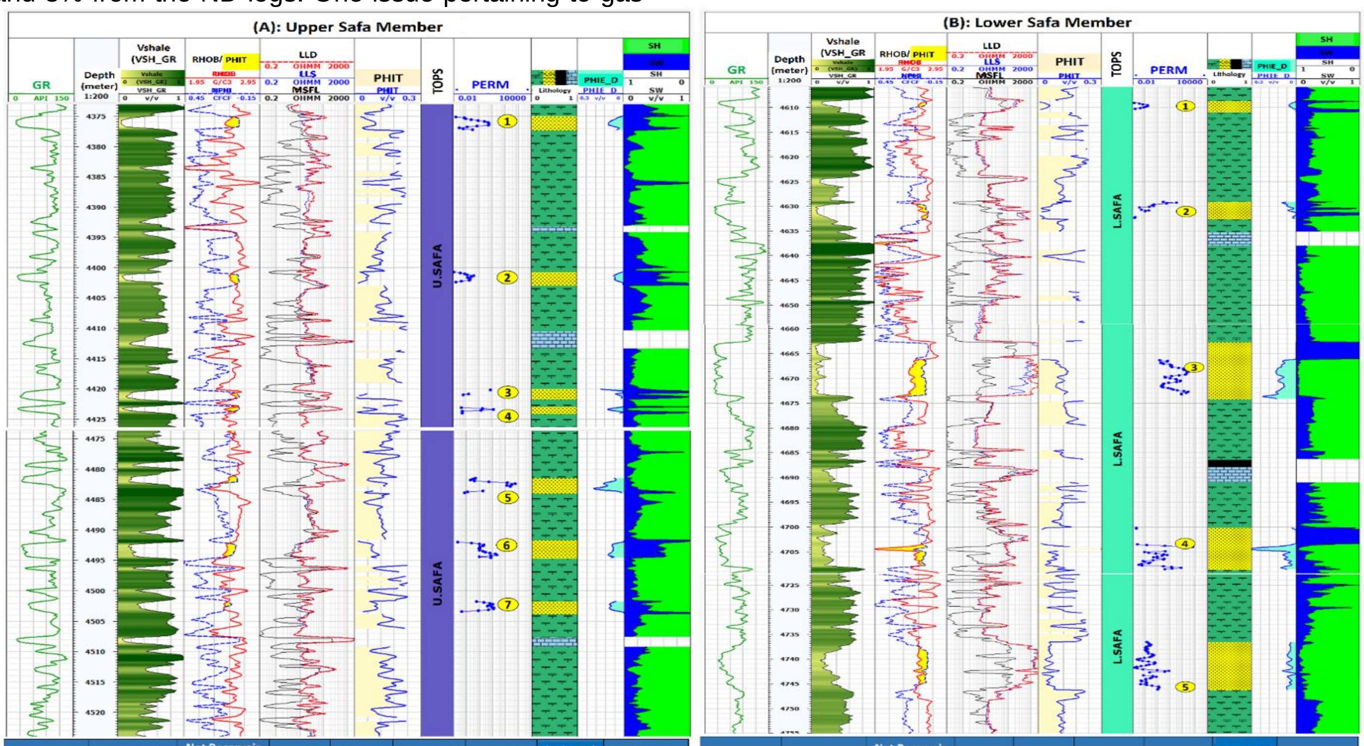

Reservoir	DEPTH (m)	Net Reservoir Thickness (m)	PHIT (%)	PHIE (%)	PERM (mD)	SW (%)	(Vsh_GR) (%)	ZONE_NAME
SAND BODY.1	4375 - 4377	2	4.00	3.00	1.74	45.01	20.00	U.SAFA
SAND BODY.2	4401 - 4403	2	3.33	4.13	0.12	62.30	26.84	U.SAFA
SAND BODY.3	4420 - 4422	2	4.00	4.04	1.24	68.98	28.11	U.SAFA
SAND BODY.4	4423 - 4424	1	3.50	4.20	2.21	39.97	26.66	U.SAFA
SAND BODY.5	4481.5 - 4483	1	4.00	3.50	25.00	11.08	40.39	U.SAFA
SAND BODY.6	4492 - 4495	3	7.00	4.00	4.18	57.58	30.00	U.SAFA
SAND BODY.7	4502 - 4503	2	4.93	3.33	5.62	39.25	40.65	U.SAFA
Average		13	4.39	3.74	5.73	46.31	30.38	U.SAFA

Reservoir	DEPTH (m)	Net Reservoir Thickness (m)	PHIT (%)	PHIE (%)	PERM (mD)	SW (%)	(Vsh_GR) (%)	ZONE_NAME
SAND BODY.1	4609- 4610	1	4.03	3.12	0.07	25	18.00	Lower Safa
SAND BODY.2	4629- 4631	2	5.77	5.06	2.97	26	13.50	Lower Safa
SAND BODY.3	4631.8- 4632.5	0.8	2	1.54	0.01	24	17.56	Lower Safa
SAND BODY.4	4666- 4673	7	10.86	10.51	61.37	11	4.01	Lower Safa
SAND BODY.5	4700- 4709	8	6.89	6.47	23.12	30	12.00	Lower Safa
SAND BODY.6	4737- 4746	10	5.60	4.48	0.76	25	9.00	Lower Safa
Average		29.15	5.90	5.20	14.72	23.47	12.35	Lower Safa

Fig. 6. The “Computed Petrophysical Interpretation” plot shows the petrophysical data of (A) the Upper Safa and (B) the Lower Safa “sandstone reservoirs." The lithosaturation panel represents the following: Track 1: gamma Ray (GR) curve; Track 2: volume of shale (Vsh); Track 3: porosity curves (density-neutron); Track 4: resistivity curves (shallow-deep-micro); Track 5: total porosity (PHIT); Track 6: permeability (PERM); Track 7: lithology; Track 8: effective porosity; Track 9: water saturation (SW) and hydrocarbon saturation (SH). The table attached to Figure 6A represents the petrophysical evaluation of the Upper Safa member, while the table attached to Figure 6B represents the petrophysical evaluation of the Lower Safa sandstone intervals.

4.3. Geomechanics results

For a correct and reliable assessment of how brittle a reservoir is, standard well logs and direct measurements of geomechanical properties like Young's modulus E and Poisson’s ratio σ must be used (Grieser and Bray, 2007; Rickman et al., 2008). The rock's brittleness increases proportionally with the magnitude of the brittleness index (BI). The analysis of the BI in conjunction with the mineralogy logs along the Imhotep W-1X well reveals that intervals characterized by elevated levels of quartz and calcite exhibit are more brittleness compared to intervals with higher clay content, which display lower levels of brittleness and higher ductility. As mentioned before, the sandstone in the Lower Safa member contains calcareous cement, which induces ductility at some intervals in the sandstone reservoirs.

Although the calcareous inter-layers are usually thin, they can be identified by combining conventional logging curves with dip logging curves, as explained by Rubing (2014). In this method, the well log responses of these thin calcareous layers can be identified as showing long and stable drilling times without hole enlargement. The Lower Safa resistivity log of the sandstones is low on the straight parts of the Middle Jurassic section of the Khatatba Formation. However, it is high in front of the calcareous inter-thin layers. This can be monitored from the microspherical focused resistivity curve (MSFL), where it is greater than 5 Ω·m. Moreover, the calcareous cemented sandstones are characterized by low natural gamma readings (20−35 API), high density (over 2.5 g/cm3), low acoustic time readings, and low neutron porosity readings of less than 8% (Rubing, 2014). A filter was applied with the curve limits to identify the calcareous cement layers. It was discovered that the severe calcareous thin layers are mostly found in the high-tightness sandstones that are held together by carbonates or anhydrites. The effect of the calcareous cement of the sandstone reservoir was also identified on the electric logs. The presence of the dogleg shape after a porous and permeable interval indicates the presence of calcareous cement, which causes low porosity and permeability (Fig. 7).

In Fig. 8, the relationship between the Poisson’s ratio and Young's modulus for the Lower Safa sandstone calcareous cement intervals is illustrated. They exhibit a moderate Poisson’s ratio and a high Young's modulus. Yet, the ductile portion of the sandstone is characterized by a high Poisson’s ratio and a moderate Young's modulus.

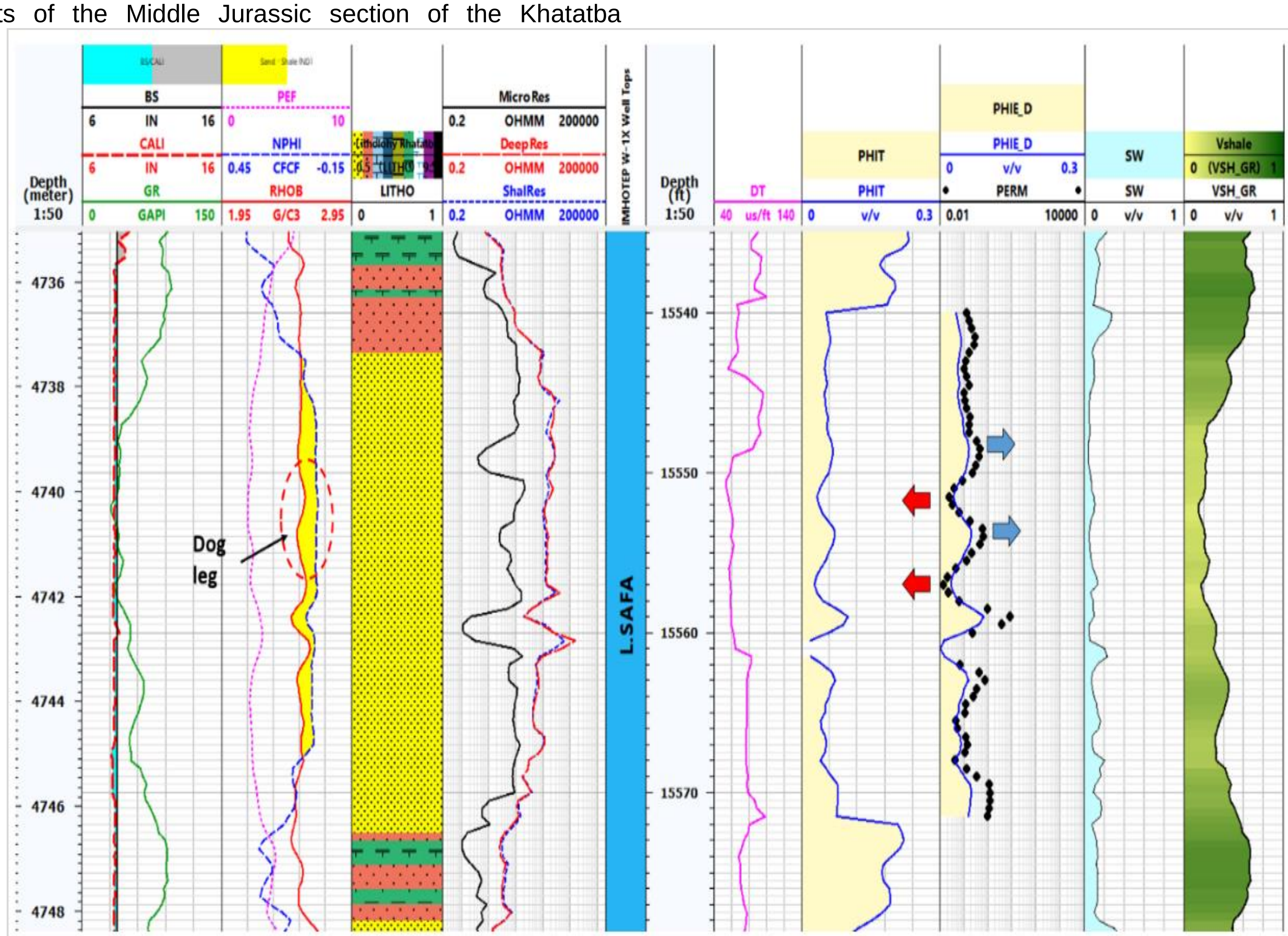

Fig. 7. The bit size (BS) and caliper (CALI) curves are almost in line with each other in front of the Lower Safa sand. A dog-leg shape indicates calcareous cement, which lowers the porosity and permeability values.

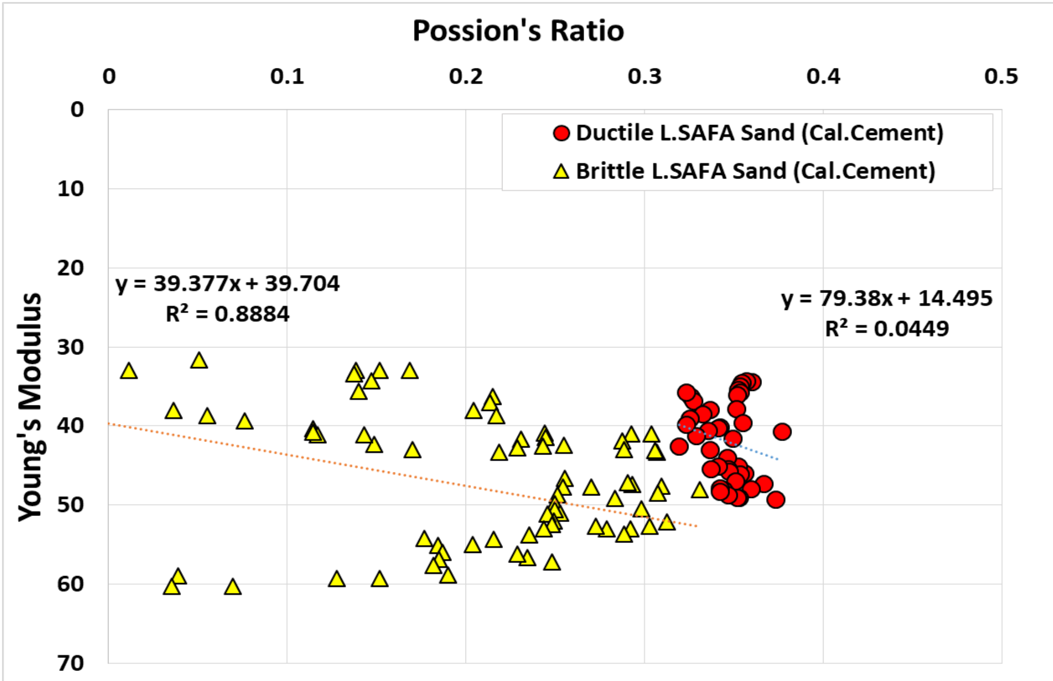

Fig. 8. Calcareous cemented-sandstone intervals of the Lower Safa member show moderate Poisson's ratio and high Young's modulus for (brittle) sand with high regression (R^2 = 0.88) while the ductile sand of Lower Safa shows weak regression (R^2 = 0.0449).

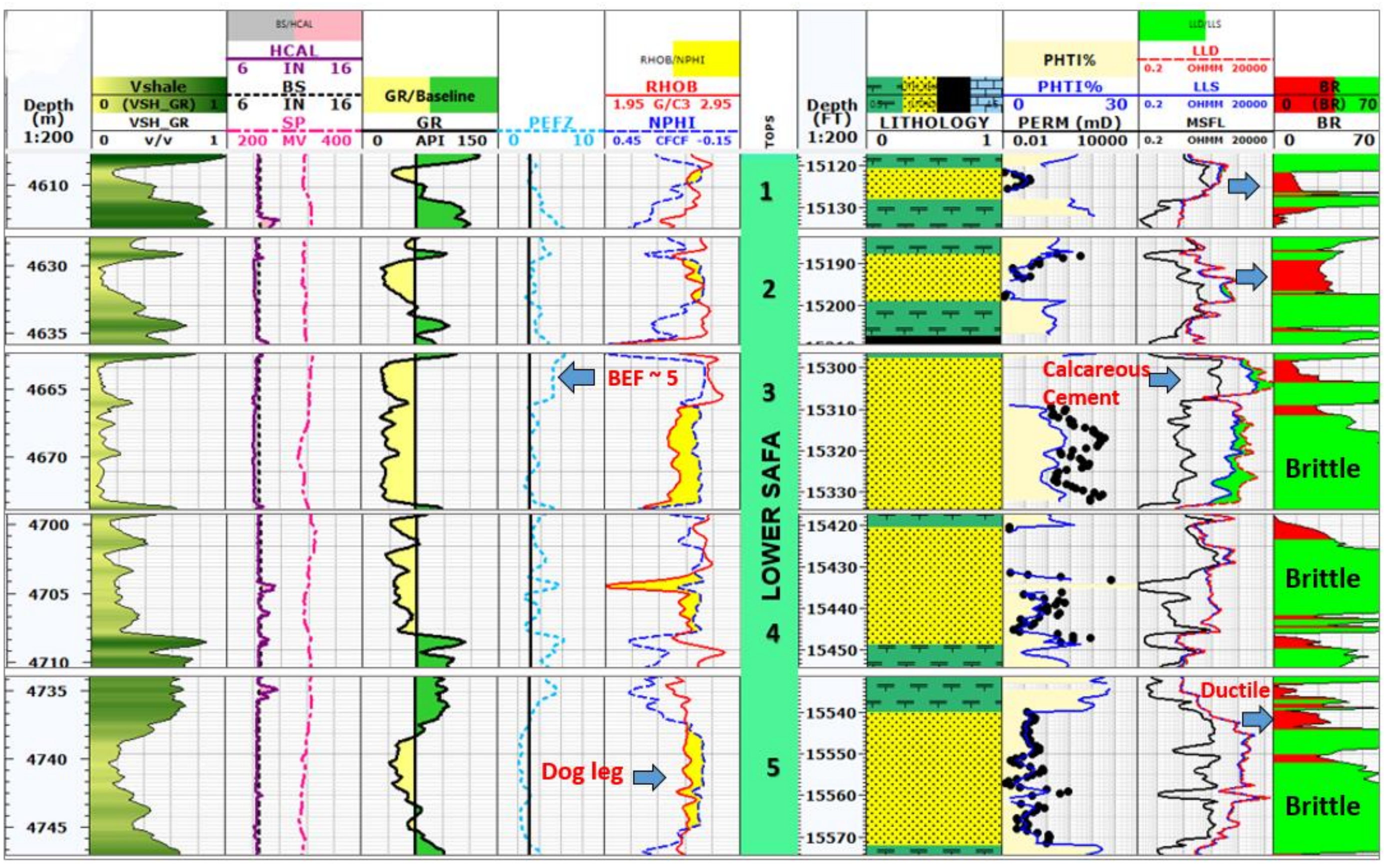

Fig. 9. The CPI "Computed Petrophysical Interpretation" plot shows the Lower Safa main sandstone reservoir units, evaluation, and brittleness index in the last track.

As seen in Figure 8, there is a positive correlation between the magnitude of the BI and the brittleness of the rock. The lithological composition of the Upper Safa has a greater tendency for brittleness as opposed to ductile characteristics.

Figure 9 demonstrates that the Lower Safa reservoir exhibits ductility in the sand body intervals due to a higher clay concentration compared to the Upper Safa member. The penetration rate almost increases linearly with an increasing rock brittleness index in the Imhotep W-1X well.

As we can see in Table 2 below, the penetration rate in the Upper Safa member is lower than that in the Lower Safa member for all lithological content. This suggests that the Lower Safa is more brittle than the Upper Safa, despite the few intervals are affected by calcareous cement and high clay content. As we can see in Figure 10 below, the ductile shale intervals are consistent with high TOC content and high GR readings, while ductile sand reservoirs are related to high clay content.

Table 2. Average penetration rate at different lithologies of the Khatatba Formation members in the Imhotep W-1 well.

Unit	Siltstone	Sandstone	Shale	Limestone	Coal
Zahra	-	-	20 ft/hr	17 ft/hr	-
Upper Safa	15 ft/hr	20 ft/hr	14 ft/hr	19 ft/hr	13 ft/hr
Kabrit	-	-	-	20 ft/hr	-
Lower Safa	21 ft/hr	25 ft/hr	16 ft/hr	23 ft/hr	30 ft/hr

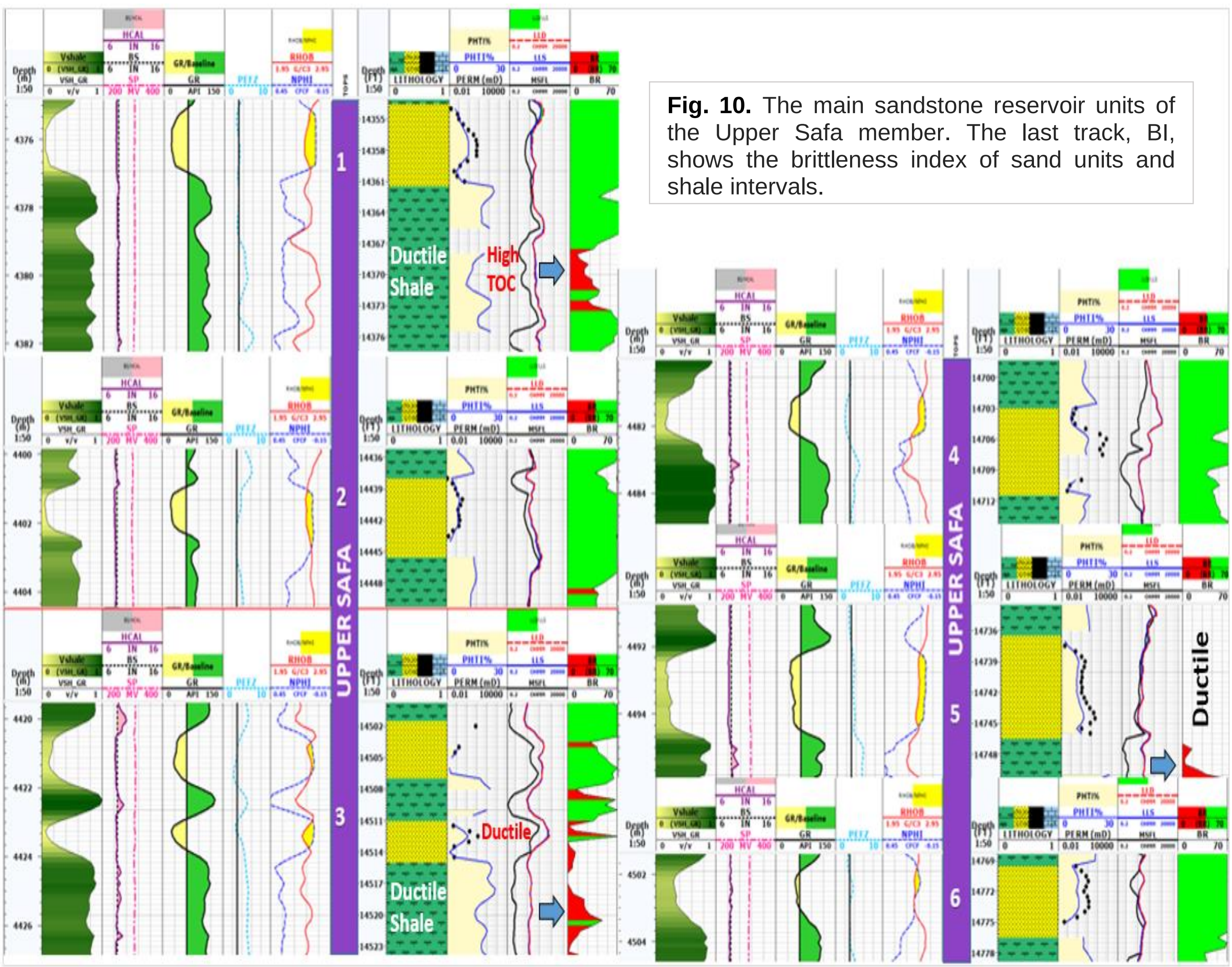

Fig. 10. The main sandstone reservoir units of the Upper Safa member. The last track, BI, shows the brittleness index of sand units and shale intervals.

Fig. 11. (a): Brittleness Index vs. Depth for different lithologies of the Upper Safa member (sand, coal, and carbonate) **(b):** Young's modulus vs. Poisson's Ratio of the shale of the Upper Safa member shows the brittle and ductile shale. **(c):** Sand of Upper Safa Reservoir Brittleness Index (Young's Modulus vs. Poisson's Ratio).

This behavior can also be monitored from the crossplot of Poisson's ratio versus the Young's modulus, as illustrated in Figures 11 b and c below. The ductile shale shows a high Poisson's ratio and a low Young's modulus. The inverse is correct for the brittle shale.

5. Discussion on the petroleum potential of the Khatatba Formation in the Imhotep W-1X well

In the early Cretaceous, shale and siltstone sealing rocks were deposited in the AEB-5 Member. This was followed by subsidence in the late Early Cretaceous, which caused the Khatatba Formation source rocks to start to mature. As a result, some oil was generated, migrated, and accumulated in the sandstone reservoirs of the Upper Safa member of the Middle Jurassic Khatatba Fm and the AEB-6 Member of the Lower Cretaceous Alam El Bueib Fm, trapped in the pre-existing Jurassic and Early Cretaceous structural traps. Even though the Lower Safa sandstones are higher in calcite cement, most of the petrophysical parameters (net effective pay, average effective porosity, average water saturation, and average hydrocarbon saturation) show that they have better reservoir parameters than the Upper Safa member. Studying the Imphotep-W-1X well's mud log indicates that the Upper Safa member has moderately sorted, moderately consolidated sand, siliceous cement, and traces of free kaolin. It has poor porosity and a higher average shale volume, with higher kaolinite percentages than those recorded from the Lower Safa member. This can be explained because it is associated with longer periods of humid climate and the deposition of high clay minerals in the Matruh basin, as explained by Ali (2023). This compositional heterogeneity, due to the high clay mineral content, downgrades the porosity and permeability of the Upper Safa member.

Operationally, the geomechanical analysis of such potential reservoirs is an essential process for the successful implementation of petroleum activities, including exploration and production. It requires a complete understanding of the brittle and ductile characteristics of the reservoir. High Young's modulus values and correspondingly low Poisson's ratio values indicate significant brittleness in the formation. Based on the geomechanical analysis, the Lower Safa member is a brittle sand reservoir that is easier to drill into than the Upper Safa member in the Khatatba Formation in the Imhotep W-1X well. It was also found that the Imhotep W-1X gas reservoir was in the Lower Cretaceous AEB-6 member of the Alam El Bueib Formation and the Middle Jurassic Lower Safa member of the Khatatba Formation. These layers were full of gas and condensates. However, the production occurred on the AEB-6 member because the pressure test showed no depletion in pressure during the production. The Lower Safa member, when tested showed a high decline in production (from 7 to 2 gas million cubic feet) and pressure depletion to 4500 psi. Therefore, the lower Safa was isolated after the pressure test. Adding to that, the deeper Lower Safa gas reservoir needs high pressure to produce gas and condensates. As a suggestion, to produce gas from the Lower Safa member, a station for gas control with a minimum number of 10–15 wells is needed. It is a production-wise process to cover the cost of a station built with gas production from the Imhotep W-1X well.

According to the preceding discussion, the Khatatba Fm in the Imhotep W-1X well proves superior reservoir characteristics. Furthermore, in order to evaluate its potential for hydrocarbon resources in the region, the Khatatba Fm's diverse source and reservoir properties must be examined in several areas within the Matruh Basin using multi-approach analyses.

Conclusion

To investigate the reservoir potential of the Middle Jurassic Khatatba Fm in Imhotep Field at the Matruh Basin, analyses were conducted through the Imhotep W-1X well. The results indicate that no pay was encountered in the Upper Safa reservoir, which is classified as a tight gas sandstone reservoir with less hydrocarbon recovery. According to the geomechanical data, the Lower Safa member is a brittle reservoir with better drilling capabilities than the more ductile Upper Safa member. The reservoir's quality was the biggest risk tested in the Imhotep field. This is because the vertical facies change, and there are low-permeability sandstone facies in the Khatatba Fm. The prospect area's Lower Safa, and Upper Safa members are shale-dominated. These shales form the top and lateral seals for the Imhotep W-1X well prospect accumulation; however, sealing is not anticipated to be a major problem. Because the Upper and Lower Safa sandstone reservoirs have different petrophysical and geomechanical properties, we need to look at other parts of the Matruh Basin and study the elements of the petroleum system to learn more about their potential to produce hydrocarbons in a regional scale.

Acknowledgements

Author is very grateful to the Egyptian General Petroleum Corporation (EGPC) and Khalda Petroleum Company for granting rock samples and well logging data for the Imhotep W-1X well.

Data availability

Data was utilized under license for the current study and are not authorized for public accessibility. Only the final tables, plates, and figures are permitted for public access and can be obtained from the corresponding author, while the initial dataset and its detailed information are restricted.

Declaration of competing interest

The author affirms that she do not possess any identifiable conflicting financial interests or personal ties that could have potentially influenced the findings presented in this paper.

References

Abdou A, (1998). Deep wells in Khalda West: a brief review. 14th EGPC Petroleum Conference, Cairo.v.2, 517–533.

Al-Areeq, N.M., Alaug, A.S., (2014). Well log analysis and hydrocarbon potential of the Sa'ar–Nayfa reservoir, Hiswah Oilfield, eastern Yemen. Arabian Journal of Geosciences 7, 2941–2956.

Ali, W. A., and Fagelnour, M. Burial and thermal history simulation of the Middle Jurassic source rocks in Matruh basin, north Western Desert, Egypt. Delta Journal of Science 47(1), 171-191 (2023).

Ali, W. A. Depositional environment and paleoclimate of the Middle Jurassic sedimentary rocks in Matruh Basin, Northwestern Desert, Egypt. Egyptian Journal of Geology 67(1), 299-319 (2023).

Ali, W.A., Deaf, A.S., Mostafa, T. 3D geological and petrophysical modeling of Alam El-Bueib formation using well logs and seismic data in Matruh field, northwestern Egypt. Sci Rep 14, 6849 (2024).

Aljahdali, M.H., Deaf, A.S., Gentzis, T., Bantan, R.A., Abu-Zied, R.H., Carvajal-Ortiz, H., Khalaf, M.M., (2023). Organic petrographic, geochemical, and sequence stratigraphic analyses for evaluating the hydrocarbon potential of Middle Jurassic–Lower Cretaceous rocks in Shushan Basin, northwestern Egypt. Frontiers in Earth Science 11:1129379.

Asquith, G. B., Krygowski, D., & Gibson, C. R. (2004). Basic well log analysis (Vol. 16, pp. 305-371). Tulsa: American Association of Petroleum Geologists.

Bosworth, W., Drummond, M., Abrams, M., Thompson, M., (2015). Jurassic rift initiation source rock in the Western Desert, Egypt – relevance to exploration in other continental rift systems. In: Petroleum Systems in “Rift” Basins, 34th Annual GCSSEPM Foundation Perkins Rosen Research Conference, Houston, pp. 13–16.

Bosworth, W., and Tari, G., (2021). Hydrocarbon accumulation in basins with multiple phases of extension and inversion: Examples from the Western Desert (Egypt) and the western Black Sea. Solid Earth Discussions 12, 59–77.

Clavier, C., Coates, G., & Dumanoir, J. (1984). Theoretical and experimental bases for the dual-water model for interpretation of shaly sands. Society of Petroleum Engineers Journal, 24(02), 153-168.

Deaf, A.S., Omran, A.A., El-Arab, E.S.Z., and Maky, A.F., (2022). Integrated organic geochemical/petrographic and well logging analyses to evaluate the hydrocarbon source rock potential of the Middle Jurassic upper Khatatba Formation in Matruh Basin, northwestern Egypt. Marine and Petroleum Geology 140:105622.

Diab, A. I., & Khalil, H. M. (2021). Quantitative assessment of the tight gas reservoirs in the Obaiyed field, Shushan Basin, NW Egypt. NRIAG Journal of Astronomy and Geophysics, 10(1), 320-332.

EGPC, (1992). Western Desert, Oil and Gas Fields, A comprehensive Overview. EGPC, 11th Petroleum Exploration Production Conference, Cairo, Egypt, 431.

EL Bastawesy M., Afify W., Barakat M., EL Gendy N., (2020). Petroleum System analyses of Middle Jurassic and early Cretaceous rocks, Matruh Basin, North Western Desert, Egypt. European Association of Geoscientists & Engineers, Conference Proceedings, 82nd EAGE Annual Conference and Exhibition, 2020, 1–5.

El Nady, M.M., Ramadan, F.S., Eysa, E.A., Said, N.M., (2016). The potentiality of hydrocarbon generation of the Jurassic source rocks in Salam-3x well, North Western Desert, Egypt. Egyptian Journal of Petroleum 25, 97–105.

El-Shorbagy, A. I., Mousa, D. A., Makled, W. A., El Din, M. Y. Z., (2023). Sequence stratigraphic modeling and organic matter distribution of Jurassic deposits in the Imhotep Field, Matruh Basin, Western Desert, Egypt. Neues Jahrbuch für Geologie und Paläontologie-Abhandlungen, 215-234.

El-Shorbagy, A. I., Mousa, D. A., Zein El-Din, M. Y., (2023). Source rock evaluation of Jurassic rock units for Imhotep field, Matruh basin, Western Desert, Egypt. Egyptian Journal of Geology, 67(1), 123-134.

Gentzis, T., Carvajal, H., Deaf, A., Tahoun, S.S., (2018). Multi-proxy approach to screen the hydrocarbon potential of the Jurassic succession in the Matruh Basin, north Western Desert, Egypt. International Journal of Coal Geology 190, 29–41.

Grieser, B., Bray, J., (2007). Identification of production potential in unconventional reservoirs. In Production and operations symposium. OnePetro.

Guiraud, R., Issawi, B., Bosworth, W., Ziegler, P.A., Cavazza, W., Robertson, A.H.F., Crasquin-Soleau, S., (2001). Phanerozoic history of Egypt and surrounding areas. Peri-Tethys Memoir 6, 469–509.

Guiraud, R., Bosworth, W., (1999). Phanerozoic geodynamic evolution of north–eastern Africa and the north–western Arabian platform. Tectonophysics 315, 73–108.

Hakimi, M.H., Shalaby, M.R., Abdullah, W.H., (2012). Diagenetic characteristics and reservoir quality of the Lower Cretaceous Biyadh sandstones at Kharir oilfield in the western central Masila Basin, Yemen. Journal of Asian Earth Sciences 51, 109–120.

Jaeger, J. C., Cook, N. G., & Zimmerman, R. (2009). Fundamentals of rock mechanics. John Wiley & Sons.

Khalda Petroleum Company, (2014). Final Report and Composite log of the Imhotep W-1X well (Cairo).

Knippel, E. P., Xiong, Q., Vargas, A. P. V., & Hampton, J. C. (2023). Measurements of elastic properties and their dependencies within a damage mechanics workflow. Rock Mechanics Bulletin, 2(4), 100083.

Metwalli, F.I., Pigott, J.D., Ramadan, F.S., El-Khadragy, A.A., Afify, W.A., (2018). Alam El Bueib reservoir characterization, Tut oil field, North Western Desert, Egypt. Environmental Earth Sciences 77, 1–21.

Meshref, W.M., (1999). Cretaceous tectonics and its impact on oil exploration in northern Egypt. Geological Society of Egypt. Special Publication 2, 199–244.

Osli, L.N., Yakub, N.Y., Shalaby, M.R., Islam, M.A., (2018). Log-based petrophysical analysis of Khatatba Formation in Shoushan Basin, North Western Desert, Egypt. Geosciences Journal 22, 1015–1026.

Passey, O.R., Moretti, F.U. and Stroud, J.D., (1990). A practical modal for organic richness from porosity and resistivity logs. American Association of Petroleum Geologists Bulletin 74, 1777–1794.

Pearson, D.L., (1984). Pollen/spores colour “standard”, ver 2. Phillips Petrol, privately distribution.

Perez Altamar, R., Marfurt, K., (2014). Mineralogy-based brittleness prediction from surface seismic data: Application to the Barnett Shale. Interpretation 24, T255–T271.

Pickel, W., Kus, J., Flores, D., Kalaitzidis, S., Christanis, K., Cardott, B.J., et al., (2017). Classification of liptinite – ICCP System 1994. International Journal of Coal Geology 169, 40–61.

Pillot, D., Deville, E., Prinzhofer, A., (2014). Identification and quantification of carbonate species using Rock-Eval pyrolysis. Oil & Gas Science and Technology – Revue d’IFP Energies nouvelles 69, 341–349.

Rickman, R., Mullen, M., Petre, E., Grieser, B., Kundert, D., (2008). A practical use of shale petrophysics for stimulation design optimization: All shale plays are not clones of the Barnett Shale. In SPE Annual Technical Conference and Exhibition, pp. SPE-115258.

Rubing, H.A.N., Qiang, L.I.U., Jiang, T., Huaimin, X., Zhaohui, X., Lei, Z., Zhang, P., (2014). Feature, origin and distribution of calcareous interlayers: A case of Carboniferous Donghe sandstone in Hade Oil Field, Tarim Basin, NW China. Petroleum Exploration and Development 41, 475–484.

Said R., (1990). The Geology of Egypt. Balkema-Rotterdam-Brookfield.

Sander, R., Pan, Z., & Connell, L. D. (2017). Laboratory measurement of low permeability unconventional gas reservoir rocks: A review of experimental methods. Journal of Natural Gas Science and Engineering, 37, 248-279.

Schlumberger, (1972). The essential of log interpretation practice. Schlumberger Ltd., France, pp. 45–67.

Schön, J. H. (2015). Physical properties of rocks: fundamentals and principles of petrophysics. Elsevier.

Shalaby, M.R., Hakimi, M.H., Abdullah, W.H., (2012). Organic geochemical characteristics and interpreted depositional environment of the Khatatba Formation, northern Western Desert, Egypt. American Association of Petroleum Geologists Bulletin 96, 2019–2036.

Shalaby, M.R., Hakimi, M.H., Abdullah, W.H., (2014). Petroleum system analysis of the Khatatba formation in the Shoushan basin, north western desert, Egypt. Arabian Journal of Geosciences 7, 4303–4320.

Shepherd, M., (2009). Factors influencing recovery from oil and gas fields.

Suggate, R.P., (1998). Relations between depth of burial, vitrinite reflectance and geothermal gradient. Journal of Petroleum Geology 21, 5–32.

Sultan, N., Halim, M.A., (1988). Tectonic framework of northern Western Desert, Egypt and its effect on hydrocarbon accumulations. In proceedings of the EGPC 9th exploration and production conference, Cairo. Egyptian General Petroleum Corporation Bulletin 2, 1–19.

Wu, W., & Grana, D. (2017). Integrated petrophysics and rock physics modeling for well log interpretation of elastic, electrical, and petrophysical properties. Journal of Applied Geophysics, 146, 54-66.

Zou, C., Mao, L., Tan, Z., Zhou, L., Liu, L., (2021). Geochemistry of major and trace elements in sediments from the Lubei Plain, China: Constraints for paleoclimate, paleosalinity, and paleoredox environment. Journal of Asian Earth Sciences 6:100071.